

## QUANTITATIVE STRESS MEASUREMENTS OF BULK MICRODEFECTS IN MULTICRYSTALLINE SILICON

S. Schoenfelder<sup>1,2,3</sup>, A. Sampson<sup>3</sup>, V. Ganapati<sup>1,3</sup>, R. Koepege<sup>1</sup>, J. Bagdahn<sup>2</sup>, T. Buonassisi<sup>3</sup>  
<sup>1</sup>Fraunhofer Institute for Mechanics of Materials, Walter-Huelse-Str. 1, 06120 Halle, Germany  
<sup>2</sup>Fraunhofer Center for Silicon Photovoltaics, Walter-Huelse-Str. 1, 06120 Halle, Germany  
<sup>3</sup>Massachusetts Institute of Technology, Cambridge, MA 02139, USA  
 stephan.schoenfelder@iwmh.fraunhofer.de

**ABSTRACT:** In this work, inclusions of silicon carbide and silicon nitride in multicrystalline silicon are investigated experimentally by photoelasticity and theoretically by numerical simulation in a finite-element model. Large tensile stresses were observed in experiment at the interface from silicon carbide to silicon while silicon nitride induced much lower stresses. The results of the finite-element model indicate that the stresses are induced while cooling during crystallization, by the mismatch of coefficients of thermal expansion.

**Keywords:** Defects, Impurities, Multicrystalline Silicon

### 1 INTRODUCTION

It is well known that crystal defects, such as dislocations or grain boundaries, and impurities, such as carbon, nitrogen, iron, or copper, can reduce the efficiencies of multicrystalline silicon (mc-Si) solar cell devices [1,2]. Less well appreciated, is the influence of defects on the mechanical properties (strength behavior) of wafers and cells, which correlates to process yield. It is thus of interest to investigate the mechanical impacts of defects in mc-Si, and the local stresses they cause.

From the structural point of view, these different defects can be observed directly and indirectly using different types of optical, electrical and mechanical tests. In this work, local stresses surrounding defects are probed using photoelasticity [3], a technique that employs a combination of optical and mechanical principles. The photoelastic effect can be used for different materials which are amorphous, e. g., glass, or crystalline, e. g., silicon. Transparency is required to apply the photoelastic method. Thus, the infrared (IR) range of the light has to be used for silicon. A comprehensive overview of IR photoelasticity is given elsewhere [4].

In this paper, inclusions of silicon carbide (SiC) and silicon nitride (Si<sub>3</sub>N<sub>4</sub>) in multicrystalline silicon are investigated by photoelasticity. Additionally, the origins of stresses at inclusions in the silicon matrix are analyzed with a finite-element (FE) model. Results of experiments and simulations are correlated and compared, and finally discussed regarding the influence on mechanical strength.

### 2 MATERIAL AND METHODS

#### 2.1 Samples

A multicrystalline block was crystallized by vertical gradient freeze technique. Regions of multiple inclusions were cut in 1 mm thick plates of the approximately dimension of (30x50)mm<sup>2</sup> with a wire saw. Then the samples were polished on both sides. Inclusions were found at the surface as well as in the volume by IR microscopy.

#### 2.2 Grey-Field Polariscopes

Photoelasticity describes the grade of birefringence due to mechanical stress in a sample. The birefringence can be measured as a change in the refraction indices for different planes of incidence by using polarized light. A

difference in the refraction indices leads to different velocities of light. Thus, the light waves traveling on the different planes are phase-shifted, resulting in an absolute retardation of one wave relative to the other. The amount of retardation is dependent on the stress state and can be written as

$$\delta = h c (\sigma_1 - \sigma_2) \quad (1)$$

This relation is known as the stress-optic law for the case of plane stress conditions ( $\sigma_3=0$ ). The retardation  $\delta$  depends on the principal stresses  $\sigma_1$  and  $\sigma_2$ , the thickness of the sample  $h$  and the relative stress-optic coefficient  $c$ . By measuring the change in polarization, the relative stresses or shear stresses can be determined. Further details on photoelasticity can be found in [3].

In this work, a grey-field polariscope GFP1400 (Stress Photonics, Inc.) is used which is described in detail in [4, 5]. The GFP1400 is a combination of a circular and plane polariscope, as it uses circular polarized light that is sent through the sample material and analyzed by a rotating linear polarizer. For silicon, the light is generated by a halogen light bulb and is filtered with a narrow band pass filter at 1100 nm. In this setup, a Goodrich InGaAs SWIR camera (SU320KTS-1.7RT) was used. To analyze the inclusions by silicon carbide and silicon nitride, a 5x magnification lens was used. Before every set of measurements, reference images without a sample were taken and subtracted from the sample image to minimize errors by polarization effects due to the lens and the setup. Results are given in values of retardation.

### 3 MODELING

For the theoretical investigations the inclusions of SiC and Si<sub>3</sub>N<sub>4</sub> in the silicon, bulk material was modeled as axisymmetric. The FE model calculates the thermo-mechanical behavior of the inclusion and the surrounding silicon after cooling from the brittle-ductile transition temperature of silicon down to room temperature. Due to the difference in material properties, residual stresses are induced.

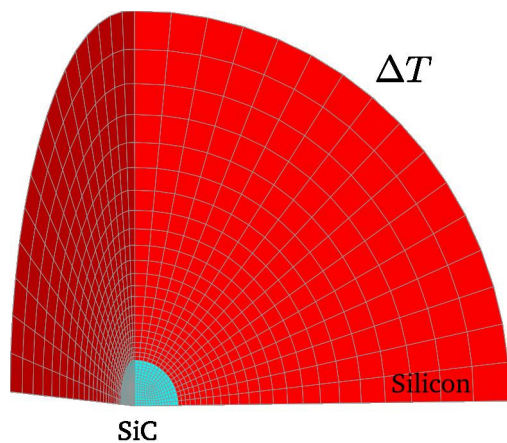
The material parameters of the silicon, SiC and Si<sub>3</sub>N<sub>4</sub> are summarized in Table 1. For all materials, linear elastic material behavior is assumed. For the elastic parameters of silicon, the anisotropic stiffness

**Table 1:** Elastic and thermal material parameters for FE models.

	Si	SiC	Si <sub>3</sub> N <sub>4</sub>
Young's Modulus [GPa]	165.9	370	300
Poisson Ratio [-]	0.217	0.188	0.24
Coefficient of Thermal Expansion [10 <sup>-6</sup> 1/K]	3.725x10 <sup>-6</sup> [1-exp[-5.88x10 <sup>-3</sup> (T-124)]] +5.548x10 <sup>-10</sup> T [T in K]	3.19x10 <sup>-6</sup> + 3.6x10 <sup>-9</sup> T -1.68x10 <sup>-12</sup> T <sup>2</sup> [T in °C]	3.1x10 <sup>-6</sup>

coefficients [6] of the cubic crystal were averaged by the method of Voigt. The variation of the coefficient of thermal expansion is taken from [7]. The elastic parameters of SiC and Si<sub>3</sub>N<sub>4</sub> were found in [8], whereas the values show larger variation than for silicon. Temperature dependent data were also used for SiC [9]. A constant coefficient of thermal expansion was assumed for Si<sub>3</sub>N<sub>4</sub>, averaged from [8].

The 3D FE model is shown in Fig. 1. Due to symmetrical reasons, only one eighth has to be modeled. The SiC inclusion is represented by a spherical shape. The bulk silicon is also modeled by a sphere with a larger diameter than the SiC inclusion. The ratio of the diameters is as large as the free surface and does not influence the result. For correct calculation of shear stress, the model can be extended to a quarter model. The model is loaded by a temperature difference  $\Delta T$ , representing the cooling from the brittle-ductile transition temperature of silicon to room temperature. The brittle-ductile transition temperature for silicon can vary between 500°C and 1000°C [7]. Below this temperature, the material behaves brittle. It can be assumed that residual stress is induced in silicon only in the brittle range. In this investigation a temperature difference of  $\Delta T=500\text{K}$  was used.

**Fig. 1:** 3D FE model of SiC inclusion in the silicon bulk material, modeled in spherical shape.

It should be noted that the calculation of the resulting stresses could also be done by a 2D axisymmetric model which is more efficient than a 3D model. However, the 2D model cannot be used for the quantitative correlation with experimental data. In order to calculate the retardation by Eq. (1) based on the stress field, the plane stresses in Cartesian coordinates have to be integrated along the path of traveling light. Furthermore, the stress-optic coefficients of silicon have to be known to correlate

stress and retardation. As the mechanical properties, the stress-optic coefficients of silicon also show anisotropic behavior. These orientation-dependent parameters were determined by various authors in literature [10-12]. Unfortunately, the results show a large variation up to 40%. In this work, an average quasi-isotropic value of  $c = 2 \times 10^{-11} \text{ Pa}^{-1}$  was used, based on the results of He [10].

#### 4 RESULTS

The results out of experiment and simulation can be compared qualitatively and quantitatively. In Fig. 2, the qualitative maps of different stress components are shown for experiment and simulation. In the sample, a region was chosen that contains a single silicon carbide cluster around a long silicon nitride rod. This is a good example to compare with the model, since no other inclusions are disturbing the stress field. As it can be seen in Fig. 2, the maximum shear stress, represented by the difference of principal stresses, fits well to the observed stress field in photoelasticity. At the interface of SiC and silicon, large tensile stresses are oriented in radial direction. Normal to the interface, the magnitude of the tensile stress strongly decreases with increasing distance. The shear stress is represented in Cartesian coordinates (the edges of the image correspond to  $x$  and  $y$  directions), thus a clover leaf stress pattern results. This shape can be found in the experiment as well as in the simulation.

Compared to a model with a SiC particle only, the model considering the Si<sub>3</sub>N<sub>4</sub> rod (cf. Fig. 2) shows no significant difference in the qualitative results of the stress fields. The stress around the Si<sub>3</sub>N<sub>4</sub> rod is much smaller than for SiC. This can be explained by the smaller CTE mismatch, which results in smaller residual stress, in agreement with experimental observations. Thus, the SiC is dominating the residual stress field around the clusters of inclusions of SiC and Si<sub>3</sub>N<sub>4</sub>.

For quantitative comparison, line scans of the maximum shear stress were taken from the experimental data. The line scans were oriented normal to the SiC/Si interface and extended from the interface into the silicon material. Line scans of different particles are shown in Fig. 3a. The result of the model is given as a range of possible values since uncertainties in material parameters, especially the stress-optic coefficient and the temperature of brittle-ductile transition, gives a strong variation in the quantitative curve. The estimated curves consider different variations in parameters. It is shown that retardations along the line scan are similar in simulation and experiment. In Fig. 3b, the calculated stress distribution along a line scan is shown. It can be seen that tensile stresses in the range of 150 MPa are induced in

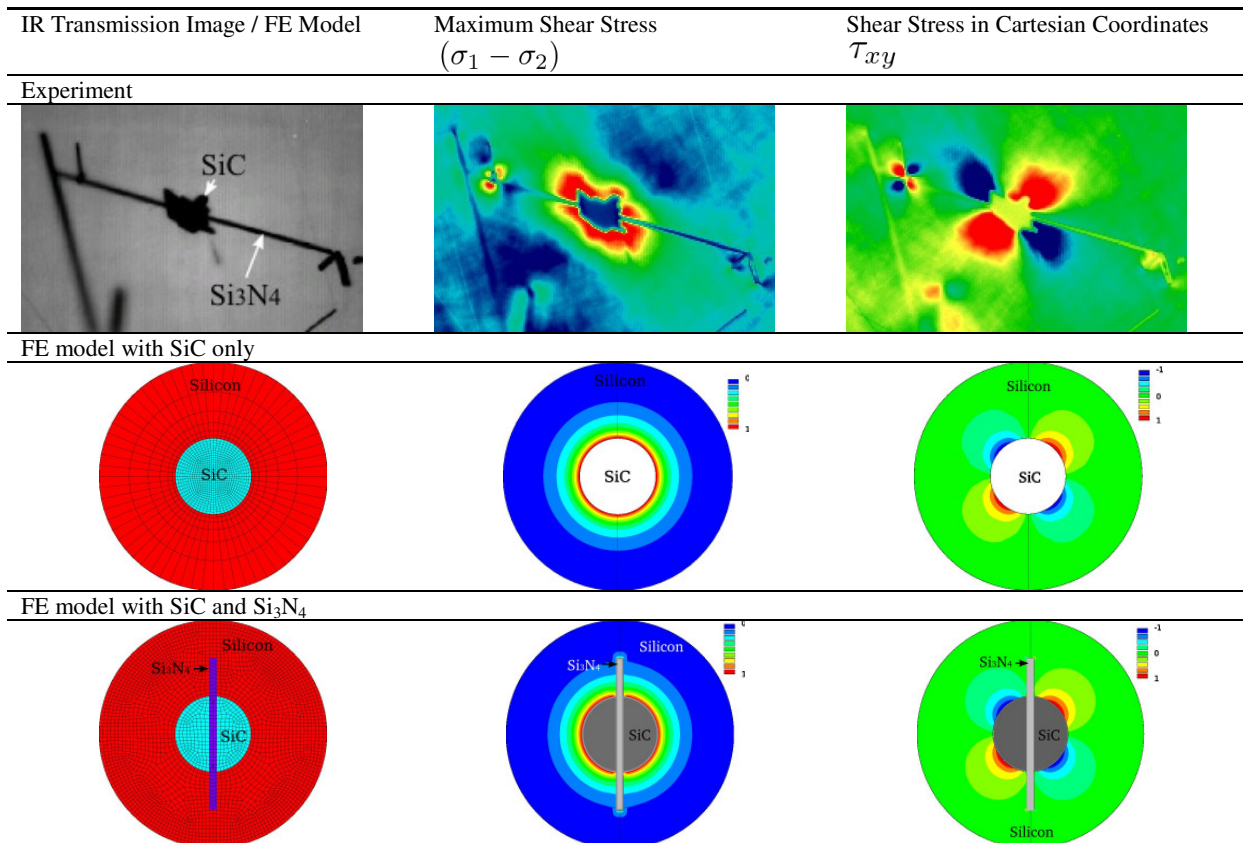


**Fig. 2:** Qualitative stress distribution in experiment and simulation for maximum shear stress and shear stress in Cartesian coordinates.

the silicon as residual stress. As the experimental results the stress decreases strongly and is vanished in a distance of  $4r$  ( $r$  is the radius of the inclusion).

### 5 DISCUSSION

The results indicate that residual tensile stress is induced in silicon around SiC and  $\text{Si}_3\text{N}_4$  clusters due to the CTE mismatch of the materials while cooling from the brittle-ductile transition temperature. Above the transition point, stresses would result in plastic deformation of the crystal and do not contribute to the

residual stress state. Interestingly, the values of residual stress are not dependent on the size of the inclusion. The tensile stresses in silicon can lead to lower fracture strength of the material since the critical fracture stress is reached by a small additional load. Hence, the inclusion of bulk defects should influence the strength of wafers and solar cells, and increase the breakage rate.

From the perspective of fracture mechanics, inclusions can be analyzed in different ways. One can differ between mechanical and thermal loads. It can be shown by analytical fracture mechanics equations [13] that an inclusion in tensile load leads only to a small

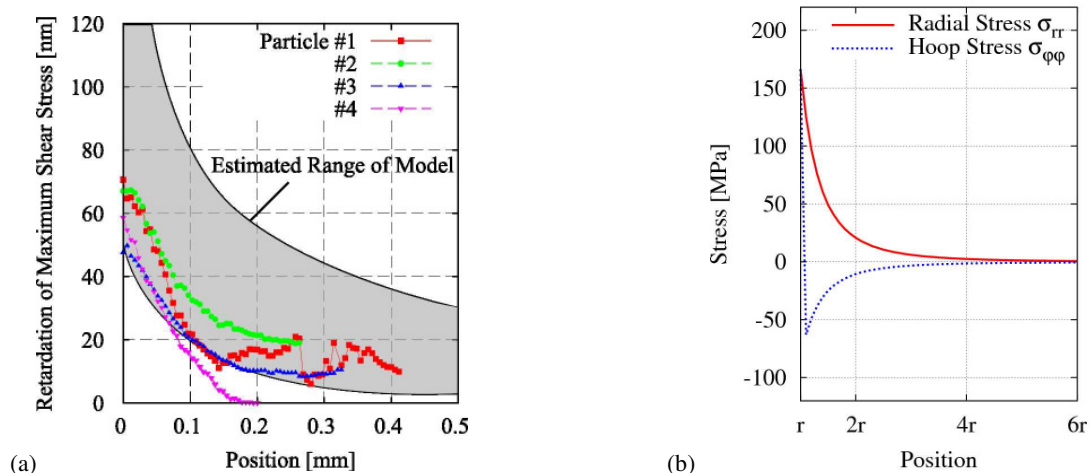


**Fig. 3:** (a) Qualitative of line scans of the maximum shear stress normal to the SiC/Si interface for experiment and FE model, (b) Radial and hoop stress along line scan normal to the SiC/Si interface in dependance of the radius of the inclusion.

stress concentration if the material of the inclusion is stiffer than the surrounding matrix material. In the case of thermal load, much higher stresses can be induced dependent on the CTE mismatch. Thus, the inclusions are most critical because of the induced residual stress while cooling.

## 6 CONCLUSIONS

In this work, the residual stress fields around inclusions of SiC and Si<sub>3</sub>N<sub>4</sub> were investigated by photoelastic measurements and FE models. While large stresses were found around SiC inclusions, Si<sub>3</sub>N<sub>4</sub> exhibited much smaller stresses. This can be explained by the difference in CTE mismatch: the SiC/Si CTE mismatch is much greater than Si<sub>3</sub>N<sub>4</sub>/Si. This model has large uncertainties because of large variations in material parameters. For a reliable quantitative correlation, more investigations, especially concerning the stress-optic coefficients, are needed.

## 7 ACKNOWLEDGEMENT

This work was partly funded by the Federal Ministry of Education and Research (BMBF) within the "Innoprofile" initiative SiThinSolar (contract no. 03IP607), and the U.S. Department of Energy under contract number DE-FG36-09GO19001. The authors want to thank Jon Lesniak (Stress Photonics, Inc.) for the fruitful discussions regarding the grey-field polariscope.

## 8 REFERENCES

- [1] Breitenstein, Bauer, and Rakotoniaina, *Material-Induced Shunts in Multicrystalline Silicon Solar Cells*, Semiconductors, 2007, 41, 440-443.
- [2] Coletti *et al.*, *Effect of iron in silicon feedstock on p- and n-type multicrystalline silicon solar cells*, Journal of Applied Physics 2008, 104, 104913.
- [3] Dally and Riley, *Experimental Stress Analysis*, McGraw-Hill, New York, 1991
- [4] Horn *et al.*, *Infrared grey-field polariscope: A tool for rapid stress analysis in microelectronic materials and devices*, Review of Scientific Instruments, 2005, 76, 1-10
- [5] Horn, *On Infrared Grey-Field Photoelasticity and Applications for Defect Detection in Bonded Semiconductor Devices*, Phd Thesis, University of Illinois at Urbana-Champaign, 2004
- [6] Hall, *Electronic Effects in the Elastic Constants of n-Type Silicon*, Phys. Rev., American Physical Society, 1967, 161, 756-761
- [7] Hull, *Properties of Crystalline Silicon*, Institution of Engineering and Technology, 1999
- [8] Alexander and Shackelford, *CRC Materials Science and Engineering Handbook*, CRC Press, 2001
- [9] Li *et al.*, *Thermal expansion of the cubic (3C) polytype of SiC*, Journal of Materials Science, 1986, 21, 4366-4368
- [10] He *et al.*, *Analysis and determination of the stress-optic coefficients of thin single crystal silicon samples*, Journal of Applied Physics, AIP, 2004, 96, 3103-3109
- [11] Iwaki *et al.*, *Stress-optic Law in a Single Crystal and Its Application to Photo-anisotropic Elasticity*, Experimental Mechanics, 1989, 29, 295-299
- [12] Giardini, *Piezobirefringence in Silicon*, The American Mineralogist, 1958, 43, 249-262
- [13] Murakami, *Stress Intensity Factors Handbook*, Great Britain: Pergamon Press, 1990